Optics Communications 439 (2019) 76–84

Contents lists available at ScienceDirect

Optics Communications

journal homepage: www.elsevier.com/locate/optcom

Compressed sensing imaging system based on improved theoretical model and its weighted iterative strategy

Yun-Hui Li [a,b,*], Xiao-Dong Wang [a], Zhi Wang [a,c]

[a] Changchun Institute of Optics, Fine Mechanics and Physics, Chinese Academy of Sciences, Changchun 130033, China
[b] University of Chinese Academy of Sciences, Beijing 100049, China
[c] Changchun UP Optotech (Holding) Co., Ltd, Changchun 130033, China

ARTICLE INFO

Keywords:
Computational imaging
Compressed sensing
Image restoration

ABSTRACT

Based on the characteristic analysis of the traditional block-based compressed sensing system, an improved compressed sensing theory model is proposed in this paper, and its hardware implementation scheme and the overall system workflow are specified according to the model requirements. Compared with the traditional block-based compressed sensing system, the linear array detector is used instead of the area array detector in the system, and the one-dimensional encoding is adopted instead of the two-dimensional encoding to simplify the encoding process. The experimental results show that the system proposed by this paper can significantly improve the image quality compared with the block-based compressed sensing system under the same system conditions, and eliminate the block effect that is common in the block-based compressed sensing system. On the basis of the proposed system, a weighted iterative restoration strategy based on frequency estimation is proposed. By adaptively adjusting the restoration process and optimizing the distribution of computing resources, the image quality is further improved.

1. Introduction

E. J. Candès et al. proposed the compressed sensing theory for the first time in 2006, which specifics that if a signal is sparse in a certain transform domain, then the original signal can be accurately recovered from a small number of measurements with high probability by solving a convex optimization problem [1–3]. This theory breaks the limitation of the traditional Nyquist–Shannon sampling theorem and greatly reduces the amount of data. It has been widely concerned in the fields of data compression [4], medical imaging [5,6], radar [7,8] and space remote sensing [9,10]. And there are also potential applications in 3D imaging [11,12] and super-resolution imaging [13,14].

Compressed sensing theory can be divided into two stages: compressed sampling and signal recovery. Therefore, there are two important technical paths for better performance: one is to optimize the measurement matrix at the sampling end to improve the sampling efficiency; the other is to propose a recovery algorithm that can obtain higher image quality in a shorter time. Amit Ashok described a hybrid measurement basis design that exploits the power spectral density statistics of natural scenes to minimize the reconstruction error by employing an optimal combination of a nonrandom basis and a purely random basis [15]. A matrix formulation in the compressed spectral imaging sensing problem has been proposed by Jonathan Monsalve, which reduces computational complexity and allows to design sensing matrices using principal components analysis, leading to improved reconstructions [16]. Abhijit Mahalanobis presented a methodology for designing a set of measurement kernels (or masks) that satisfy the photon constraint and are optimum for making measurements that minimize the reconstruction error in the presence of noise [17]. By solving an equality-constrained optimization problem, Jun Ke obtained a binary sensing matrix, which has a smaller dynamic range requirement to system sensors under the similar reconstruction performance [18]. The signal recovery algorithms mainly include the basis pursuit (BP) algorithm [19], the gradient projection for sparse reconstruction (GPSR) algorithm [20], Total Variation(TV) Minimization [9], etc., and their various improved forms.

If the compressed sensing theory is introduced into the imaging system, it is indispensable to give a hardware implementation based on its theoretical model. The coded sampling methods that have been proposed in the compressed sensing imaging system mainly include Digital Micromirror Devices (DMD) [21,22], moving random exposure [23], charge transfer random exposure [24], Complementary Metal Oxide Semiconductor (CMOS)-based approach [25], etc., among which DMD is the most commonly used at present. M. F. Duarte proposed a DMD-based single-pixel camera as the first hardware-implemented compressed sensing imaging system [21]. However, both the encoding time and the image reconstruction time increase rapidly as the image size increases,

* Corresponding author at: Changchun Institute of Optics, Fine Mechanics and Physics, Chinese Academy of Sciences, Changchun 130033, China.
E-mail address: liyunhui_ciomp@126.com (Y.-H. Li).

https://doi.org/10.1016/j.optcom.2019.01.050
Received 11 September 2018; Received in revised form 17 January 2019; Accepted 20 January 2019
Available online 23 January 2019

so the practicality is limited. In order to overcome this problem, a block-based compressed sensing imaging system has been proposed by John P. Dumas, in which an area array detector is used instead of the single-pixel sensor, and the image is processed in parallel blocks, which effectively reduces the sampling and reconstruction time [22].

On the basis of block-based compressed sensing system, in order to further improve the image quality, several adaptive sampling and image recovery methods are proposed. The main idea is to predict the characteristics of the imaging target and then take adaptive processing to different regions of the target, thereby improving image quality under limited resources. Ying Yu proposed a saliency-based compressed sampling scheme for image signals. The key idea is to exploit the saliency information of images, and allocate more sensing resources to salient regions but fewer to non-salient regions [26]. Based on the fact that low frequency components are relatively more crucial to the perceptual quality of images than high frequency components, Yi Yang proposed a novel sampling scheme for compressed sensing framework by designing a weighting scheme for the sampling matrix [27]. By taking full advantage of the characteristics of the block-based compressed sensing, Zheng Hai-bo presented a sampling adaptive block compressed sensing strategy, which assigns a sampling rate depending on its texture complexity of each block [28].

Whether it is the optimization of measurement matrix and recovery algorithm in compressed sensing theory, or the implementation scheme of hardware system, and the adaptive processing of coded sampling and recovery strategy, the essence are all based on the theoretical model of compressed sensing. The model itself has not been optimized to accommodate the two-dimensional imaging field.

The basic model of compressed sensing theory is mainly for one-dimensional signals. If the theory is introduced into the imaging system, the two-dimensional image needs to be integrated into a one-dimensional signal first, and then the theoretical model of compressed sensing and the corresponding restoration algorithm can be applied mechanically. Such processing obviously weakens the sparsity of the signal in a certain transform domain, which is the foundation of compressed sensing theory, thus limiting the improvement of imaging quality in the compressed sensing system. In view of the above problem, we have established a theoretical model of compressed sensing based on two-dimensional image signal architecture, and also proposed an implementation scheme of hardware system based on this model.

Compared with the block-based compressed sensing system, the compressed sensing system proposed by this paper adopts one-dimensional coding mode and replaces the area array detector with linear array detector. Furthermore, on the basis of the proposed system, a weighted iterative restoration strategy based on frequency estimation is proposed. By adaptively adjusting the restoration process and optimizing resource allocation, the image quality is further improved.

The main innovations of this paper are summarized as follows:

(a) Based on compressed sensing theory, the improved compressed sensing theoretical model for two-dimensional images is established.

(b) The implementation scheme of the hardware system is proposed for the above model, and the correspondence with the model is specified.

(c) A weighted iterative restoration strategy based on frequency estimation is proposed on the basis of the above model, which optimizes the restoration process, improves the image quality.

The rest of this paper is organized as follows. The characteristics of the block-based compressed sensing system are analyzed in Section 2. In Section 3, we established the improved theoretical model of compressed sensing, and proposed an implementation scheme of hardware system based on this model. On the basis of the proposed system, the weighted iterative restoration strategy based on frequency estimation is proposed in Section 4, and the overall system composition and imaging workflow are also presented. Experimental verification and data analysis are completed in Section 5. After summarizing the above contents, the conclusion is given in Section 6.

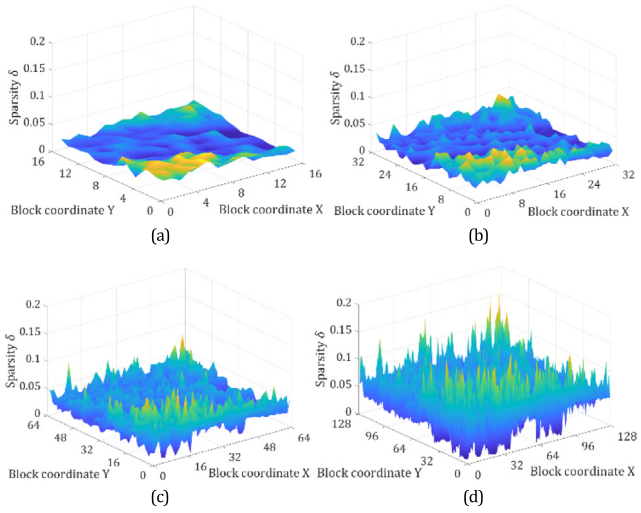

Fig. 1. Distribution of the sparsity δ under different number of blocks. (a) 16×16, (b) 32×32, (c) 64×64, (d) 128×128.

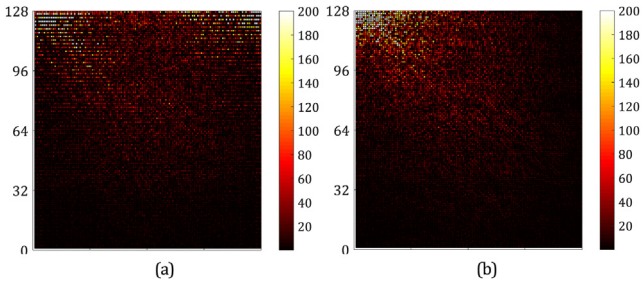

Fig. 2. Sparse matrix maps with different sparse basis transformation. (a) One-dimensional DCT, (b) Two-dimensional DCT.

2. Characteristic analysis of block-based compressed sensing system

Based on the bottleneck of matrix size and computational complexity in practical imaging applications, the block-based compressed sensing system is proposed to process image blocks in parallel, which shortens the encoding time and reduces the time of image restoration. But the problems that come with it are:

(a) After being processed by blocks, the image's integrity is weakened, so that the sparsity of each image block is deteriorated. As shown in Fig. 1, for a target image with a resolution of 2048×2048, the discrete cosine transform (DCT) base is used for block-based sparse transform. The ratio of the number of elements larger than a certain threshold in the sparse vector to the size of the whole vector is defined as the sparsity δ. As the number of blocks increases, the number of pixels in each block gradually decreases, and the sparsity δ also deteriorates significantly. Therefore, the block processing of the block-based compressed sensing system will result in a degradation in the quality of the restored image, and there will also be some mosaic block effect.

(b) From the above-mentioned transformation relationship between the actual sampling process and the theoretical model, it can be known that the original two-dimensional image needs to be reorganized into a one-dimensional signal in the theoretical model, which also destroys the natural property of the image as a two-dimensional signal, resulting in further deterioration of the sparsity. Taking the Lena image with a resolution of 128×128 as an example, the one-dimensional DCT transform and the two-dimensional DCT transform are performed respectively, and the obtained sparse matrices are shown in Fig. 2.

It can be seen from Fig. 2 that the significant elements of the sparse matrix transformed by one-dimensional DCT are mainly concentrated in the upper half of the matrix, while the significant elements of the sparse matrix transformed by two-dimensional DCT are mainly concentrated in the upper left corner of the matrix, and it is obvious that the latter has fewer significant elements and a better matrix sparsity. Therefore, if the integration process from two-dimensional image signal to one-dimensional signal is removed, and the two-dimensional image signal is directly applied to the compressed sensing theory model for processing, then the sparsity of the matrix can be improved after two-dimensional sparse transformation, thereby improving the imaging quality.

3. Improved compressed sensing theory and imaging system

3.1. The improved theoretical model of compressed sensing

The traditional compressed sensing theory is mainly aimed at one-dimensional signals, which has more or less limitations for imaging systems whose target is two-dimensional image. Based on this, if the target image is regarded as a two-dimensional signal matrix $X \in \mathbb{R}^{N\times N}$, and the sparse representation after two-dimensional transformation is $\Theta \in \mathbb{R}^{N\times N}$, then there is $X = \Psi^{\mathrm{T}}\Theta\Psi$, where Ψ is a sparse basis. The measurement matrix is $\Phi \in \mathbb{R}^{M\times N}$ and the sampling result matrix is $Y \in \mathbb{R}^{M\times N}$. The entire coded sampling process can be expressed as:

$$Y = \Phi X = \Phi\Psi^{\mathrm{T}}\Theta\Psi \tag{1}$$

Since Ψ is an orthogonal matrix, there is $\Psi^{\mathrm{T}} = \Psi^{-1}$, and the above equation can be further organized as:

$$Y' = Y\Psi^{\mathrm{T}} = \Phi\Psi^{\mathrm{T}}\Theta = \Omega\Theta \tag{2}$$

where $Y' \in \mathbb{R}^{M\times N}$ is called the equivalent two-dimensional sampling result matrix, and the two-dimensional sensing matrix $\Omega = \Phi\Psi^{\mathrm{T}}$.

Since the two-dimensional matrix cannot be restored directly, the above equation needs to be split by column, then Y' can be expressed as:

$$Y' = [Y'_{c1} \quad Y'_{c2} \quad \cdots \quad Y'_{cN}] \tag{3}$$

And Θ can be expressed as:

$$\Theta = [\Theta_{c1} \quad \Theta_{c2} \quad \cdots \quad \Theta_{cN}] \tag{4}$$

Then Eq. (11) can be disassembled as:

$$Y'_{ci} = \Omega\Theta_{ci}(i = 1 \ldots N) \tag{5}$$

Each of the above sub-equations can be iteratively calculated by solving the following optimization problems:

$$\hat{\Theta}_{ci} = \arg\min_{\Theta_{ci}\in\mathbb{R}^N} \|\Theta_{ci}\|_{\ell 1} \quad \text{subject to } Y'_{ci} = \Omega\Theta_{ci}(i = 1 \ldots N) \tag{6}$$

A total of N sets of iterative calculations are required. After acquiring the sparse vectors $\hat{\Theta}_{ci}$, they will be integrated into a two-dimensional sparse matrix $\hat{\Theta}$, and then the restored target image $\hat{X}$ can be obtained by the following equation:

$$\hat{X} = \Psi^{\mathrm{T}}\hat{\Theta}\Psi \tag{7}$$

3.2. Compressed sensing imaging system

According to the above compressed sensing theory model, the hardware implementation scheme is presented here. The compressed sensing system based on the improved model is similar to the block-based compressed sensing system. As shown in Fig. 3, the hardware structure is mainly composed of the imaging target, the front-end optical lens, the coded aperture, the back-end optical lens and the linear array detector. The incident light passes through the front-optical lens, the coded aperture template, the back-end optical lens successively, and finally reaches the focal plane of the detector.

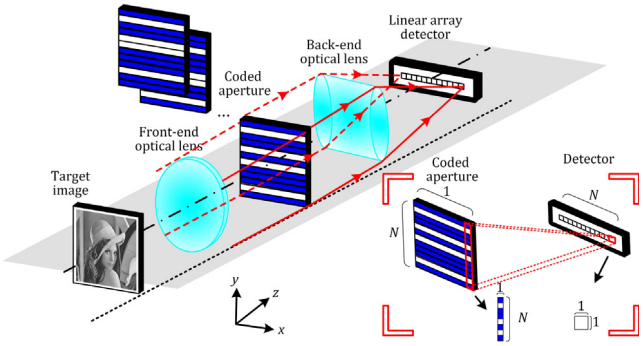

Fig. 3. The composition of compressed sensing imaging system based on the improved model.

Unlike the block-based compressed sensing system, the coded aperture in the system is one-dimensionally coded along the y-axis direction in the figure, and the optical signal is focused on the linear array detector through the back-end optical lens after being encoded by the aperture. There is a strict correspondence between the detector and the coded aperture template, and one detector pixel corresponds to one column of the coded aperture template. If the size of the whole image is $N \times N$, then the size of the coded aperture template is $N \times 1$ and the pixel number of the linear array detector is $1 \times N$.

It is assumed that the target image is matrix $X \in \mathbb{R}^{N\times N}$, the sampling result of the detector is vector $E(p) \in \mathbb{R}^N(p = 1 \ldots m)$, and the encoded template is vector $C(p) \in \mathbb{R}^N(p = 1 \ldots m)$, in which p represents the p-th encoding, then the entire coded sampling process can be expressed as:

$$\begin{bmatrix} E(1) \\ E(2) \\ \vdots \\ E(m) \end{bmatrix} = \begin{bmatrix} C(1) \\ C(2) \\ \vdots \\ C(m) \end{bmatrix} \cdot X \tag{8}$$

Then the elements of the measurement matrix Φ in the theoretical model are organized as follows:

$$\Phi = \begin{bmatrix} C(1) & C(2) & \cdots & C(m) \end{bmatrix}^{\mathrm{T}} \tag{9}$$

The elements of the sampling result matrix Y in the theoretical model are organized as follows:

$$Y = \begin{bmatrix} E(1) & E(2) & \cdots & E(m) \end{bmatrix}^{\mathrm{T}} \tag{10}$$

After the above matrix corresponding transformation is completed, the image restoration can be performed according to the proposed theoretical model.

3.3. System comparison and supplementary explanation

Compared with the block-based compressed sensing imaging system, the system adopts one-dimensional encoding method, which simplifies the system complexity.

If the ratio between the amount of sampled data and the total amount of image data is defined as the compression ratio η, the number of coded sampling m_b in the block-based compressed sensing system can be expressed as:

$$m_b = \eta \times (r \times c) \tag{11}$$

And the number of coded sampling m_t in the system proposed in this paper can be expressed as:

$$m_t = \eta \times N \tag{12}$$

It can be seen that the number of coded sampling of both are proportional to the compression ratio. The number of coded sampling in block-based compressed sensing system is independent of the overall

image size, and is only related to the size of each block. The larger the size of each block, the more the number of sampling is required. The number of sampling in this paper is only related to the overall image size.

It should be noted here that it seems that the compressed sensing imaging system proposed only encodes and samples each column of the target image during the sampling process, and does not directly acquire all the pixel information of the two-dimensional image. However, due to the two-dimensional sparse transformation of the target image in the theoretical model, it can be seen from Eq. (2) that when the system model is organized into the standard form of the compressed sensing theory, each element of Y' as the equivalent sampling result matrix has realized the aliasing and sampling of all the pixels in the two-dimensional image, so the coverage of image information collection is theoretically guaranteed, which ensures the effectiveness of the method.

4. Weighted restoration strategy

4.1. The necessity of image restoration optimization

The real-time performance of image acquisition is an important technical index in imaging system. The acquisition time of a single image in compressed sensing imaging system mainly includes coded sampling time, data processing and transmission time, and image restoration time. The process of image restoration occupies a lot of time, which is the decisive factor affecting the real-time performance of the system. The time of image restoration is closely related to the number of iterations which can be verified in the following experimental results. Therefore, it is worth exploring how to obtain a higher quality image in the case that the total number of iterations is constant during the image restoration process. Or from another point of view, how to reduce the number of iterations and thus shorten the restoration time in the same image quality.

4.2. Weight coefficient generation method

In order to improve the image restoration quality within a limited time, we consider assigning different weights to the iterative restoration process of each column under the framework of the compressed sensing system proposed above. It can be seen from Fig. 2 of Section 2 that after the two-dimensional DCT transform, the significant elements of the sparse matrix are mainly concentrated in the upper left corner of the matrix. Therefore, with the column number increasing, the frequency component of the signal represented by the element gradually increases, and the value decreases rapidly. Based on the above analysis, more restoration weights should be given to columns with smaller column number in the sparse matrix. In addition, from the perspective that the human eye is more sensitive to low-frequency information, the same approach should be taken.

Based on this, we propose a weight coefficient generation method based on frequency distribution estimation. The main idea is to obtain the first column restoration results of sparse matrix, and then estimate other columns of sparse matrix according to the results of this column, and finally the moduli of other columns are taken as their own weight coefficients. The specific method is described as follows:

In the sparse matrix Θ after two-dimensional DCT transformation, the different elements $\theta_{i,j}$ represent the amplitudes of the different frequency signals contained in the image. If the magnitudes of the same frequency components in the image are considered to be substantially identical, as shown in Fig. 4, the other columns of the sparse matrix can be approximately equivalent to the known first column, that is, the elements in the same color in the figure are equivalent. Although each column has more elements at the bottom of the column vector than the equivalent elements in the first column, the element value drops sharply as the frequency gradually increases, so this part is negligible.

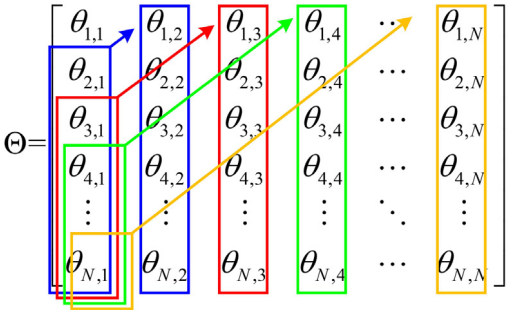

Fig. 4. The schematic diagram of element equivalent in sparse matrix.

According to the above equivalent analysis, the modulus of each column can be approximated as:

$$\left\|\Theta_j\right\| = \sqrt{\sum_{i=1}^{N}\theta_{i,j}^2} \approx \sqrt{\sum_{i=1}^{N}\theta_{j+(i-1),1}^2} \approx \sqrt{\sum_{i=1}^{(N+1)-j}\theta_{j+(i-1),1}^2}(j=2\ldots N) \quad (13)$$

It can be known from the above estimation algorithm that the moduli of other columns can be estimated as long as the elements in the first column are obtained, and thus we can get the weight coefficient of each column. The algorithm implementation flow is presented as follows:

Step1: The sampling result matrix Y is known, and Y' can be calculated according to the equation $Y' = Y\Psi^{\mathrm{T}}$.

Step2: Calculating $\hat{\Theta}_{c1}$ according to Eq. (6), wherein the number of iterations is the maximum value $S_{\max}$.

Step3: Calculating $\left\|\Theta_j\right\|(j=2\ldots N)$ according to Eq. (13).

Step4: Weight coefficient $W_j = 20\log(\left\|\Theta_j\right\| + 1)(j=2\ldots N)$.

4.3. Weight distribution strategy

The more iterations, the more time it takes, but the higher the quality of the restored image. Based on the above premise, the image restoration time can be equivalently converted to the total number of iterations according to the computational performance of the system, and then the number of iterations in each column is determined by the weight coefficient.

Assuming that the total number of iterations is I, the maximum number of iterations for each column is set to $S_{\max}$, and the minimum number of iterations is $S_{\min}$, then the number of iterations per column can be calculated according to the flow shown in Fig. 5.

First, the initial iterations of each column are calculated based on weight coefficients.

$$I_j = (I - S_{\max}) \cdot \frac{W_j}{\sum_{j=2}^{N} W_j}(j=2\ldots N) \quad (14)$$

Then, the number of iterations for each column is constrained according to the maximum and minimum iterations.

$$I_j = \begin{cases} S_{\max} & I_j > S_{\max} \\ S_{\min} & I_j < S_{\min} \\ \mathrm{round}(I_j) \end{cases} \quad (15)$$

Furthermore, the relationship between the total number of iterations and the given values is summarized.

$$\Delta = \frac{I_r - I_r'}{I_r}(I_r' = \sum_{j=2}^{N} I_j) \quad (16)$$

where δ is a small constant. If $|\Delta| > \delta$, Eq. (17) is executed, and the result is returned to Eq. (15). The process is reiterated until $\Delta \le \delta$ is satisfied, then the whole iteration process is finished, and I_j is output as the number of iterations per column.

$$\begin{cases} S_{\min} = S_{\min} \cdot (1+\Delta) \\ I_j = I_j \cdot (1+\Delta) \end{cases} \quad (17)$$

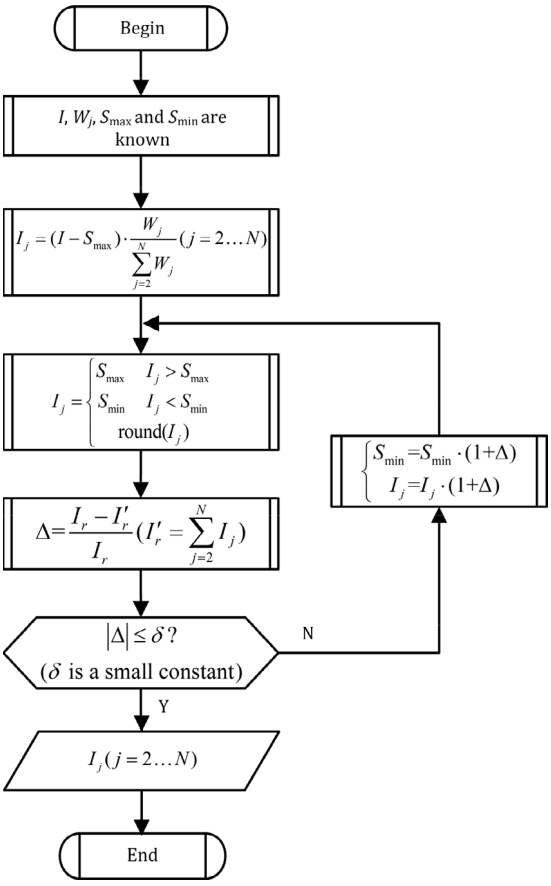

Fig. 5. The flowchart for generating the number of iterations per column.

4.4. The overall framework and workflow of the system

Taking the improved compressed sensing imaging system applied in the field of space remote sensing as an example, the whole system composition and workflow are shown in Fig. 6. The system on the satellite platform mainly performs compression coded sampling of the target, which is realized by the electric control box to complete the driving control of the coded aperture and the data acquisition of the linear array detector, and then the data is transmitted to the ground station via the air-ground transmission chain. Both the weighted iterative algorithm and the image restoration are performed by the computer on the ground station.

Firstly, the first column $\hat{\Theta}_{c1}$ of the sparse matrix is restored according to the received data Y, and the weight coefficient of each column W_j is generated based on the weight coefficient generation method described in Section 4.2, and then the number of iterations for each column I_j is obtained according to the weight distribution strategy described in Section 4.3, which will guide the subsequent iterative restoration. After the restoration of each column of the sparse matrix $\hat{\Theta}_{ci}$ is completed, it is integrated with the first column $\hat{\Theta}_{c1}$ into a complete sparse matrix $\hat{\Theta}$, so that the final restored image can be obtained according to Eq. (7).

In the conventional imaging system, the wireless data transmission can also be replaced by a wired data interface, the system on the satellite platform and the ground station can also be integrated into an integrated imaging control and data processing system, but the whole internal data flow and algorithm remain the same.

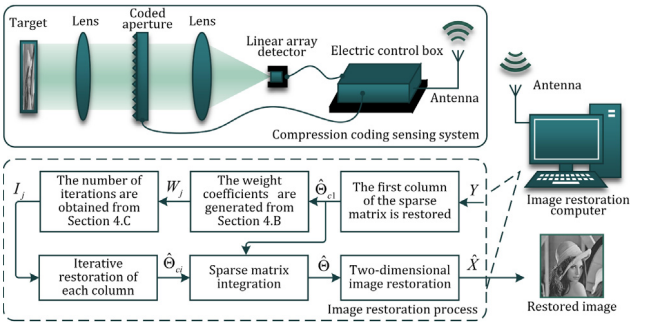

Fig. 6. The hardware composition and workflow of the improved compressed sensing imaging system.

5. Experimental results and analysis

In order to verify the effectiveness of the theoretical model, system and restoration strategy proposed in this paper, the simulation experiment environment is built based on Intel i5 dual-core processor and Matlab R2017a software platform.

The target images include people, scenes and other types with a resolution of 256 × 256. Under the premise of this parameter, the pixel number of linear array detector in the compressed sensing system proposed in this paper is 256, while the pixel number of area array detector in the block-based compressed sensing system is related to the number of blocks, which is selected as 256 here, and each block has a size of 16 × 16 for a convenient comparison with the former.

In the experimental system, the DCT basis is selected as the sparse transform base, and the orthogonal matching pursuit (OMP) algorithm is used for image restoration. Considering the implementation limitation of the coded aperture, the random Bernoulli matrix is selected as the measurement matrix.

In order to quantitatively evaluate the quality of the restored image, three image quality assessment criteria are adopted, including peak signal to noise ratio (PSNR), structural similarity (SSIM), and feature similarity (FSIM). Among them, PSNR is the most commonly used method in image quality assessment, which simply compares the pixel gray value of reference image and restored image, so it is not always consistent with human subjective feeling. Based on the fact that human visual system is good at extracting the structure information in the scene, SSIM assesses the image by evaluating the degradation of the structural information in the restored image, mainly including the comparison of the brightness, contrast and structure information. From the perspective that the human visual system mainly understands the image based on low-level features in the image (such as step edge, zero-crossing edge, etc.), FSIM extracts image phase consistency information and image gradient information, and effectively acquires features of human interest.

Through the above three image quality evaluation criteria, we can give a more objective and comprehensive quality evaluation to the restored image.

5.1. Parametric analysis of image restoration quality

In order to verify the universal applicability of the proposed model and system, four target images are selected for experiment. The mean value of 100 experimental results was used as the final output in order to eliminate the randomness of measurement matrix.

First of all, the effects of compression ratio and number of iterations on imaging quality were analyzed in the non-weighted compressed sensing system based on the improved model. Figs. 7 and 8 show the restored images of Lena and Boat under different compression ratios and iterations, respectively. Intuitively, the restored image quality of both improve with the increase of compression ratio. And when the

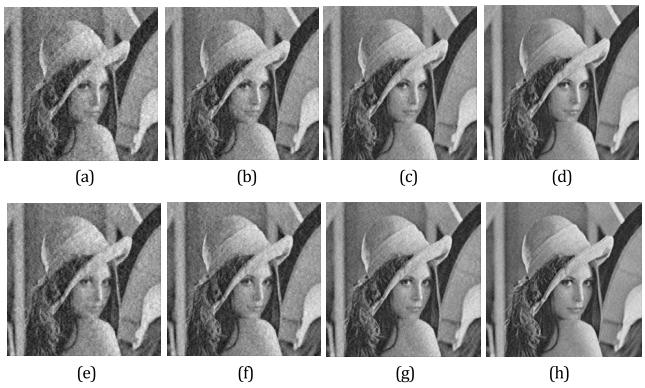

Fig. 7. The restored images of Lena under different parameters. The number of iterations is 256 × 80 in (a), (b), (c), and (d), where the compression ratio varies from 0.5 to 0.8. The number of iterations is 256 × 120 in (e), (f), (g), and (h), where the compression ratio varies from 0.5 to 0.8.

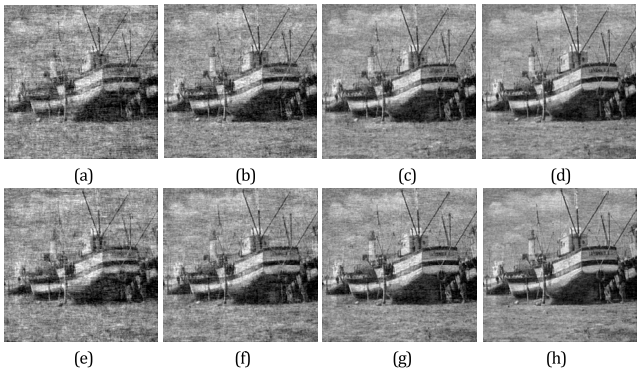

Fig. 8. The restored images of Boat under different parameters. The number of iterations is 256 × 80 in (a), (b), (c), and (d), where the compression ratio varies from 0.5 to 0.8. The number of iterations is 256 × 120 in (e), (f), (g), and (h), where the compression ratio varies from 0.5 to 0.8.

same compression ratio is adopted, the image quality improves with the number of iterations increasing.

The specific experimental results under different parameters are recorded in Table 1. From the overall trend, the image quality of the four targets improved with the increase of compression ratio and number of iterations, which is consistent with the subjective evaluation results.

Only some of the data is recorded in the above table, and more comprehensive experimental results are drawn in Figs. 9 and 10. Since the results of the three quality assessment criteria are consistent, PSNR will be used as the representative of image quality for the following analysis. It can be seen from Fig. 9 that the quality of all types of images has the same trend with the compression ratio and number of iterations, and the peaks are obtained at the highest compression ratio and the maximum number of iterations.

However, the PSNR obtained by different types of images is not the same, and the PSNR of Lena and Pepper is higher, while the PSNR of Boat and House is lower. This is mainly due to the fact that the images of Lena and Peppers are simpler than those of the latter, the frequency components are concentrated in the middle and low frequency bands, and the information such as high frequency texture is less, thus achieving better image quality.

The relationship between the PSNR and the compression ratio for the four images is plotted in Fig. 10, when different number of iterations are taken. On the one hand, PSNR increases gradually with the increase of compression ratio. On the other hand, the more the number of iterations, the higher the PSNR of the image, and with the increase of compression ratio, the PSNR increase due to the increase in the number of iterations becomes more significant.

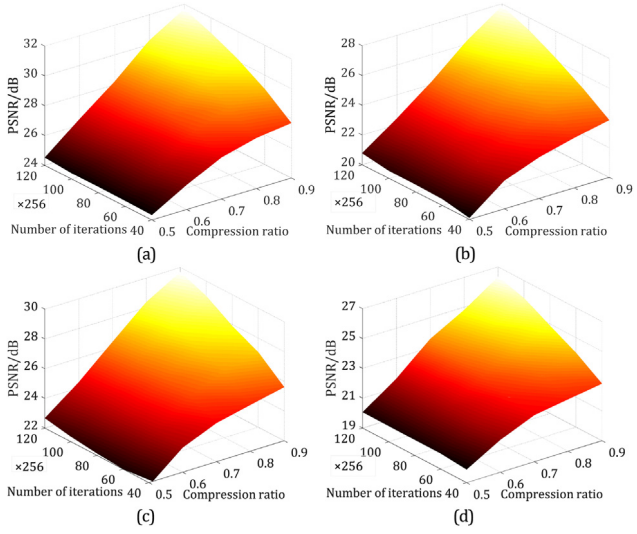

Fig. 9. The PSNR of the restored images varies with the compression ratio and the number of iterations. (a) Lena, (b) Boat, (c) Peppers, (d) House.

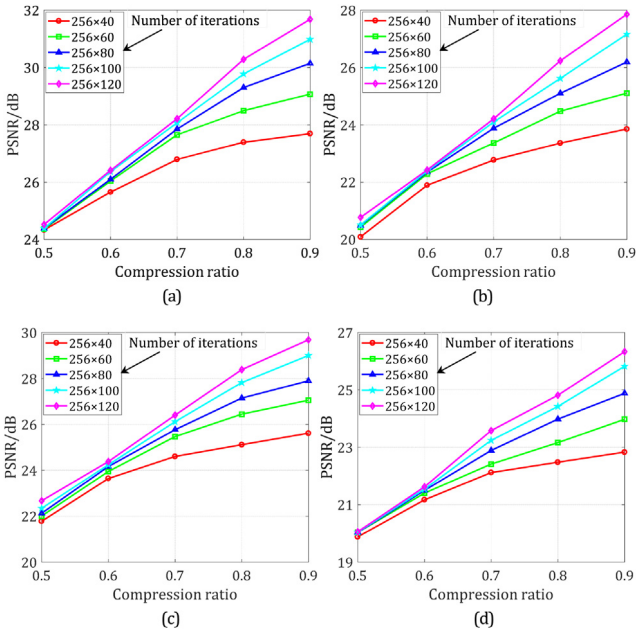

Fig. 10. The relationship between the PSNR of the restored images and the compression rate, when taking different number of iterations. (a) Lena, (b) Boat, (c) Peppers, (d) House.

5.2. The results of the weight distribution strategy

On the basis of the proposed compressed sensing imaging system, the weighted processing method proposed in Section 4 is used to optimize the distribution of the iterations for each column in the sparse matrix, and the results are shown in Fig. 11. With the Lena image as the target, the compression ratio is 0.8, and the number of iterations varies from 256 × 40 to 256 × 140 with a total of six curves drawn in the figure. It can be seen from the curves that the number of iterations decreases gradually with the increase of the column number. As the number of iterations increases, the overall curve rises, and the minimum number of iterations also increases, which are in accordance with the design idea of the algorithm strategy.

Table 1
The experimental results of the four images at different compression ratios and number of iterations.

Images	Number of iterations	256 × 40			256 × 80			256 × 120		
	Compression ratio	PSNR (dB)	SSIM	FSIM	PSNR (dB)	SSIM	FSIM	PSNR (dB)	SSIM	FSIM
Lena	0.5	24.33	0.9460	0.7745	24.39	0.9470	0.7744	24.52	0.9494	0.7676
	0.6	25.65	0.9603	0.8059	26.10	0.9647	0.8096	26.41	0.9670	0.8193
	0.7	26.79	0.9695	0.8395	27.85	0.9762	0.8540	28.21	0.9781	0.8616
	0.8	27.39	0.9733	0.8512	29.30	0.9829	0.8855	30.28	0.9864	0.9047
	0.9	27.69	0.9752	0.8621	30.14	0.9859	0.9041	31.68	0.9901	0.9294
Boat	0.5	20.09	0.8536	0.7122	20.49	0.8679	0.7216	20.77	0.8747	0.7253
	0.6	21.89	0.9021	0.7553	22.35	0.9143	0.7684	22.42	0.9156	0.7758
	0.7	22.77	0.9196	0.7796	23.88	0.9386	0.8067	24.21	0.9443	0.8176
	0.8	23.36	0.9301	0.7953	25.10	0.9537	0.8380	26.23	0.9645	0.8580
	0.9	23.85	0.9370	0.8060	26.19	0.9640	0.8589	27.85	0.9756	0.8923
Peppers	0.5	21.78	0.9264	0.7149	22.13	0.9322	0.7254	22.67	0.9389	0.7482
	0.6	23.64	0.9509	0.7738	24.16	0.9574	0.7745	24.38	0.9593	0.7850
	0.7	24.60	0.9608	0.7998	25.77	0.9703	0.8241	26.40	0.9744	0.8291
	0.8	25.11	0.9649	0.8141	27.14	0.9784	0.8481	28.38	0.9836	0.8748
	0.9	25.61	0.9687	0.8277	27.89	0.9817	0.8682	29.68	0.9879	0.9019
House	0.5	19.88	0.8533	0.7220	20.04	0.8655	0.7347	20.06	0.8641	0.7375
	0.6	21.17	0.8920	0.7545	21.50	0.9009	0.7699	21.62	0.9038	0.7723
	0.7	22.12	0.9123	0.7744	22.89	0.9269	0.8104	23.58	0.9336	0.8261
	0.8	22.48	0.9183	0.7887	23.98	0.9435	0.8322	24.81	0.9532	0.8521
	0.9	22.83	0.9247	0.7967	24.88	0.9532	0.8507	26.33	0.9716	0.8803

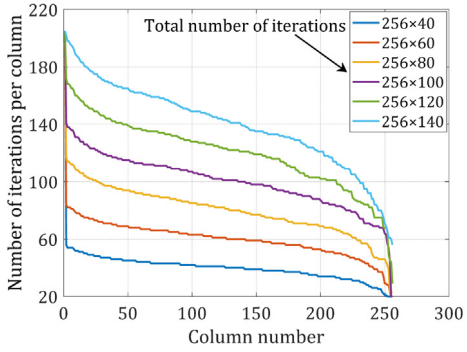

Fig. 11. The results of the number of iterations per column under different total iterations.

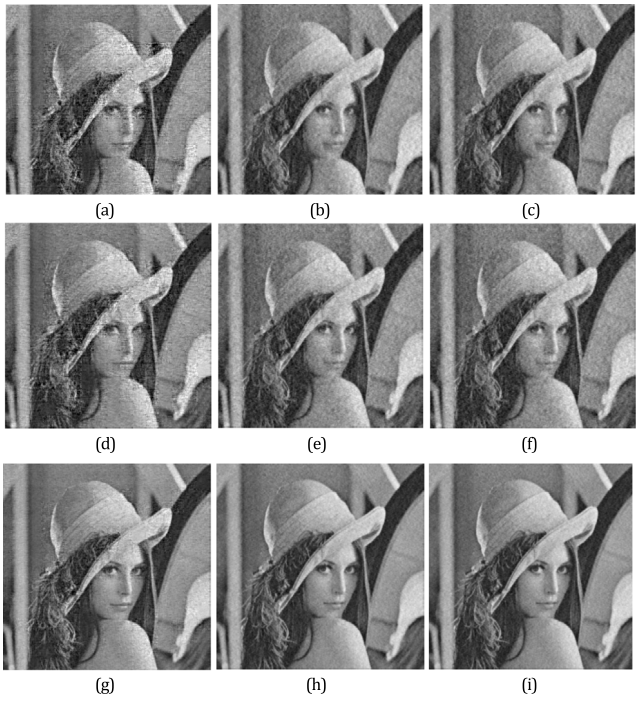

Fig. 12. The restored images obtained by the three methods. Each set of images from left to right are the results obtained by using BCS, ICS, and WICS methods, respectively. The number of iterations is 256 × 80 and the compression ratio is 0.6 in (a), (b), (c), which are 256 × 120 and 0.6 in (d), (e), (f), and 256 × 120 and 0.8 in (g), (h), (i).

5.3. Image restoration quality comparison when using different methods

In order to evaluate the performance of the proposed system and weighted iterative restoration strategy, the traditional block-based compressed sensing imaging system (BCS), the improved compressed sensing imaging system (ICS) and the improved compressed sensing imaging system with weighted iterative strategy (WICS) are compared and analyzed by experimental results.

In order to eliminate the randomness of the measurement matrix, the same generated measurement matrix is applied to the three methods simultaneously, which ensures the comparison of the three is performed under the same measurement matrix, avoiding the inequality due to the randomness of the measurement matrix. Meanwhile, the mean value of 100 experimental results was also used as the final output in order to eliminate the randomness of measurement matrix.

Taking the Lena image as an example, the restored images under different parameters are shown in Fig. 12. Each set of images from left to right are the results obtained by using BCS, ICS, and WICS methods, respectively. Intuitively, WICS is superior to ICS, and ICS is superior to BCS. And the system proposed by this paper eliminates the block effect existing in the BCS system.

The detailed experimental results under different parameters are recorded in Table 2. For further comparing the effects of the three methods on image quality, the color map of PSNR is drawn in Fig. 13, where the x-axis represents the compression ratio and the y-axis represents the number of iterations. To facilitate comparison of the three methods, the color bars in the three sub-figures are in the same range of values. The color maps in the figure from left to right are obtained by using BCS, ICS, and WICS methods, respectively. It can be seen from the figure that ICS is significantly better than BCS, and WICS has a slight improvement compared with ICS.

When the compression ratio is constant, the relationship between the PSNR of the restored image and the number of iterations are shown in Fig. 14. PSNR increases with the increase of iterations, and there are always the results that WICS is better than ICS, and ICS is better than BCS under all compression ratio conditions.

When the number of iterations is constant, the relationship between the PSNR of the restored image and the compression ratio are shown in Fig. 15. PSNR increases with the increase of the compression ratio,

Table 2
The experimental results obtained by the three methods under different compression ratios and number of iterations.

Compression ratio	Number of iterations Imaging system	256 × 40 PSNR (dB)	256 × 80 PSNR (dB)	256 × 120 PSNR (dB)
0.5	BCS	20.88	21.32	21.74
	ICS	24.33	24.39	24.52
	WICS	24.34	24.43	24.67
0.6	BCS	23.19	23.52	24.04
	ICS	25.65	26.10	26.41
	WICS	25.70	26.19	26.52
0.7	BCS	24.39	25.53	25.96
	ICS	26.79	27.85	28.21
	WICS	26.92	27.97	28.38
0.8	BCS	24.81	26.96	27.98
	ICS	27.39	29.30	30.28
	WICS	27.71	29.60	30.44
0.9	BCS	25.21	27.77	29.25
	ICS	27.69	30.14	31.68
	WICS	28.13	30.36	31.81

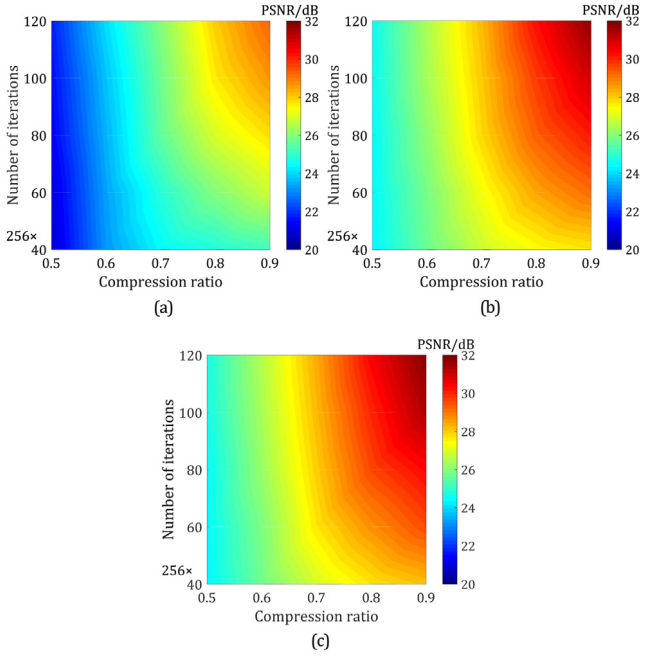

Fig. 13. The PSNR's color map of the three methods. (a) BCS, (b) ICS, (c) WICS.

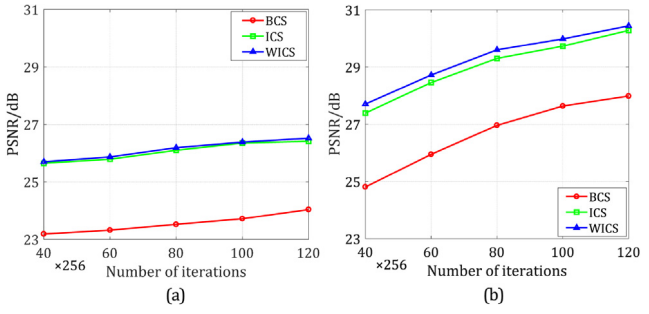

Fig. 14. The relationship between the PSNR of the restored images and the number of iterations, when taking different compression ratios. (a) The compression ratio is 0.6, (b) The compression ratio is 0.8.

and there are always the results that WICS is better than ICS, and ICS is better than BCS under all number of iterations.

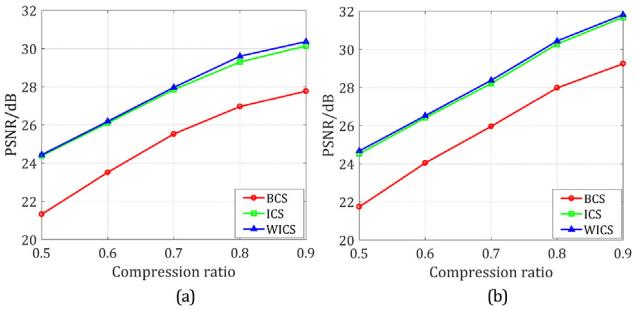

Fig. 15. The relationship between the PSNR of the restored images and the compression ratios, when taking different number of iterations. (a) The number of iterations is 256 × 80, (b) The number of iterations is 256 × 120.

Table 3
The restoration time (in seconds) of the three methods under different iterations.

Number of iterations	256 × 40	256 × 60	256 × 80	256 × 100	256 × 120
BCS	1.1490	2.1441	3.7688	6.0522	8.9329
ICS	1.1136	2.1648	3.7781	6.0331	9.2703
WICS	1.2118	2.3116	4.0366	6.3516	9.5195

According to the above analysis, the compressed sensing imaging system proposed in this paper is significantly better than the traditional block-based compressed sensing imaging system under the same parameters. And by using the weighted iterative restoration strategy, the quality of the restored image is further improved. However, when the weighted restoration strategy is adopted, the weight coefficient generation and the number of iterations generation are added in the image restoration process, which will inevitably result in the increase of image restoration time, thus having a certain negative impact.

5.4. Analysis of image restoration time

In the case of different compression ratios, the computational complexity of the restoration process is also different because of different matrix sizes. In order to quantitatively compare the time costs of the three methods, the verification is performed on the above-mentioned software and hardware platform, and the restoration time of the three methods under different iterations is recorded in Table 3 when the compression ratio is 0.8. The relationship between the restoration time and the number of iterations is plotted in Fig. 16.

It can be seen from Fig. 16 that the restoration time is positively correlated to the number of iterations. At the same number of iterations, the time consumption of BCS and ICS is basically the same, and that of WICS is slightly longer. According to the previous analysis, the weighted restoration strategy in WICS takes a little time, thus causing the above phenomenon. On the one hand, it is verified that it is feasible to equate the restoration time with the number of iterations in the above analysis. On the other hand, the time consumed by the weighted processing algorithm accounts for a very low proportion of the total restoration time, and does not vary significantly with the increase of the number of iterations. Therefore, it is meaningful to exchange this small time cost for a further improvement of image quality.

6. Conclusions

Based on the traditional compressed sensing theory model, an improved compressed sensing theory model is proposed in this paper, and its hardware implementation scheme and the overall system workflow are specified. Compared with the traditional block-based compressed sensing system, one-dimensional encoding is adopted instead of the two-dimensional encoding to simplify the encoding process. The experimental results show that the system proposed by this paper can significantly

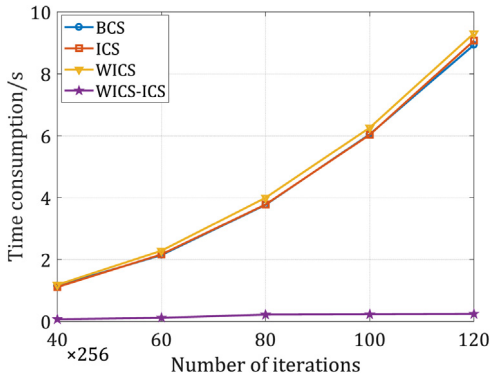

Fig. 16. The relationship between the time consumption and the number of iterations.

improve the image quality compared with the block-based compressed sensing system under the same system conditions, and eliminate the block effect that is common in the block-based compressed sensing system. On the basis of this proposed system, a weighted iterative restoration strategy based on frequency estimation is proposed, which further improves the image quality with extremely small time cost. The method and system proposed in this paper are more cost-effective than the traditional block-based compressed sensing system, and provide a better solution for the realization of the compressed sensing imaging system.

Acknowledgment

This work was supported by the Strategic Priority Research Program of Chinese Academy of Sciences, China (Grant No. XDA17010205).

References

[1] Emmanuel J. Candès, Justin Romberg, Terence Tao, Robust uncertainty principles: exact signal reconstruction from highly incomplete frequency information, IEEE Trans. Inform. Theory 52 (2) (2006) 489–509.
[2] David L. Donoho, Compressed sensing, IEEE Trans. Inform. Theory 52 (4) (2006) 1289–1306.
[3] Joel A. Tropp, Jason N. Laska, Marco F. Duarte, Justin K. Romberg, Richard G. Baraniuk, Beyond nyquist: efficient sampling of sparse bandlimited signals, IEEE Trans. Inform. Theory 56 (1) (2010) 520–544.
[4] Shuyuan Zhu, Bing Zeng, Moncef Gabbouj, Adaptive reweighted compressed sensing for image compression, IEEE Int. Symp. Circuits Syst. 30 (2014) 1–4.
[5] Christian G. Graff, Emil Y. Sidky, Compressive sensing in medical imaging, Appl. Opt. 54 (8) (2015) 23–44.
[6] David J. Brady, Alex Mrozack, Ken Maccabe, Patrick Llull, Compressive tomography, Adv. Opt. Photonics 7 (4) (2015) 756–813.
[7] Daniel J. Lum, Samuel H. Knarr, John C. Howell, Frequency-modulated continuous-wave LiDAR compressive depth-mapping, Opt. Express 26 (12) (2018) 15420–15435.
[8] Nathan A. Goodman, Lee C. Potter, Pitfalls and possibilities of radar compressive sensing, Appl. Opt. 54 (8) (2015) 1–13.
[9] S. Vishnukumar, M. Wilscy, Single image super-resolution based on compressive sensing and improved TV minimization sparse recovery, Opt. Commun. 404 (2017) 80–93.
[10] James E. Fowler, Compressive pushbroom and whiskbroom sensing for hyperspectral remote-sensing imaging, in: IEEE International Conference on Image Processing, 2015, pp. 684–688.
[11] Wen-Kai Yu, Xu-Ri Yao, Xue-Feng Liu, Long-Zhen Li, Guang-Jie Zhai, Three-dimensional single-pixel compressive reflectivity imaging based on complementary modulation, Appl. Opt. 54 (3) (2015) 363–367.
[12] Huidong Dai, Guohua Gu, Weiji He, Ling Ye, Tianyi Mao, Qian Chen, Adaptive compressed photon counting 3D imaging based on wavelet trees and depth map sparse representation, Opt. Express 24 (23) (2016) 26080–26096.
[13] Yair Rivenson, Adrian Stern, Bahram Javidi, Single exposure super-resolution compressive imaging by double phase encoding, Opt. Express 18 (14) (2010) 15094–15103.
[14] Vladimir Farber, Yitzhak August, Adrian Stern, Super-resolution compressive imaging with anamorphic optics, Opt. Express 21 (22) (2013) 25851–25863.
[15] Amit Ashok, Mark A. Neifeld, Compressive imaging: hybrid measurement basis design, J. Opt. Soc. Amer A 28 (6) (2013) 1041.
[16] Jonathan Monsalve, Jorge Bacca, Henry Arguello, Compressive sensing matrix design using principal components analysis, Comput. Opt. Sens. Imag. CTh1B.4 (2017).
[17] Abhijit Mahalanobis, Mark Neifeld, Optimizing measurements for feature-specific compressive sensing, Appl. Opt. 53 (26) (2014) 6108–6118.
[18] Jun Ke, Edmund Y. Lam, Fast compressive measurements acquisition using optimized binary sensing matrices for low-light-level imaging, Opt. Express 24 (9) (2016) 9869–9887.
[19] Scott Shaobing Chen, David L. Donoho, Michael A. Saunders, Atomic decomposition by basis pursuit, SIAM J. Sci. Comput. 20 (1) (1998) 33–61.
[20] MAT. Figueiredo, RD. Nowak, SJ. Wright, Gradient projection for sparse reconstruction: application to compressed sensing and other inverse problems, IEEE J. Sel. Top. Sign. Proces. 1 (4) (2008) 586–597.
[21] Marco F. Duarte, Mark A. Davenport, Dharmpal Takhar, Jason N. Laska, Ting Sun, Kevin F. Kelly, Richard G. Baraniuk, Single-pixel imaging via compressive sampling, IEEE Signal Process. Mag. 25 (2) (2008) 83–91.
[22] John P. Dumas, Muhammad A. Lodhi, Waheed U. Bajwa, Mark C. Pierce, Computational imaging with a highly parallel image-plane-coded architecture: challenges and solutions, Opt. Express 24 (6) (2016) 6145–6155.
[23] Guangming Shi, Dahua Gao, Xiaoxia Song, Xuemei Xie, Xuyang Chen, Danhua Liu, High-Resolution imaging via moving random exposure and its simulation, IEEE Trans. Image Process. 20 (1) (2011) 276–282.
[24] Yun-Hui Li, Xiao-Dong Wang, Zhi Wang, A novel super-resolution imaging method based on TDI CCD charge transfer and random exposure, Opt. Commun. 426 (2018) 170–181.
[25] Javad Ghasemi, Manish Bhattarai, Glauco R.C. Fiorante, Payman Zarkesh-Ha, Sanjay Krishna, Majeed M. Hayat, CMOS approach to compressed-domain image acquisition, Opt. Express 25 (4) (2017) 4076–4096.
[26] Ying Yu, Bin Wang, Liming Zhang, Saliency-based compressive sampling for image signals, IEEE Signal Process. Lett. 17 (11) (2010) 973–976.
[27] Yi Yang, Oscar C. Au, Lu Fang, Xing Wen, Weiran Tang, Perceptual compressive sensing for image signals, in: Proc ICME, 2009, pp. 89–92.
[28] Zheng Hai-bo, ZHU. Xiu-chang, Sampling adaptive block compressed sensing reconstruction algorithm for images based on edge detection, J. China Univ. Posts Telecommun. 20 (3) (2013) 97–103.